

Solution-Based Assembly of Metal Surfaces by Combinatorial Methods

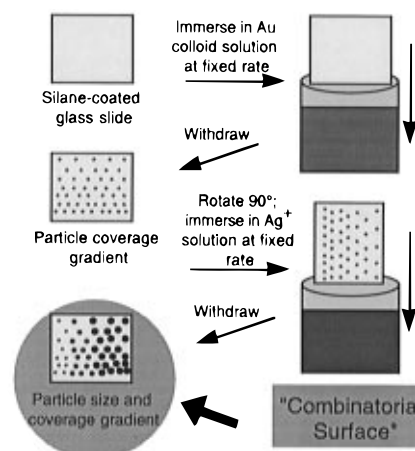
Bonnie E. Baker,[†] Nicole J. Kline,[‡] Patrick J. Treado,[‡] and Michael J. Natan^{*†}

Department of Chemistry
The Pennsylvania State University
152 Davey Laboratory
University Park, Pennsylvania 16802-6300
Department of Chemistry
University of Pittsburgh
314 Chevron Science Center
Pittsburgh, Pennsylvania 15260

Received April 22, 1996

Generation of combinatorial libraries has become an essential tool in synthetic organic chemistry,¹ but only recently have these methods been used for rapid screening of materials properties of inorganic substances.^{2,3} The initial report described the use of vapor deposition and masking techniques to vary the composition of multi-metal superconducting materials;² more recently, a similar mask-driven approach to spatially-selective vapor deposition led to discovery of materials exhibiting colossal magnetoresistance.³ Compared to traditional routes to property optimization in mixed-metal systems, e.g. preparation of separate samples with varying metal ratios,⁴ combinatorial methods potentially offer significant advantages in speed and cost. We recently described a new approach to fabrication of macroscopic Au surfaces that is based on self-assembly of nanosized Au particles from solution.^{5,6} Reductive deposition of Ag onto these substrates leads to Ag-clad colloidal Au arrays⁷ that exhibit an increased enhancement factor (EF) for surface enhanced Raman scattering (SERS).⁸ We describe herein a new, solution-based combinatorial strategy for synthesis of surfaces exhibiting nanometer-scale variation in mixed-metal composition and architecture. With this method, continuous or stepped gradients in the size and number density of surface features can be generated simultaneously over different regions of a single substrate. To demonstrate this approach, we have optimized the SERS response of a glass slide upon which the coverage of

Scheme 1. Solution-Based Combinatorial Surfaces



colloidal Au and the extent of Ag coating were varied. Over a 2 cm × 2 cm sample area, changes in EF spanning almost three orders of magnitude were realized, and the changes in nanostructure responsible for these effects were elucidated using atomic force microscopy (AFM). Our results show significant changes in SERS EFs over small alterations in surface morphology, demonstrating the power of solution-based combinatorial approaches for synthesis of mixed-metal materials.

The general combinatorial assembly approach is described in Scheme 1. Prior work has shown that the number of colloidal Au particles bound to functionalized surfaces can be predicted from immersion times in colloidal solution using initial (time)^{1/2} kinetics.⁹ Thus, when a (3-mercaptopropyl)trimethoxysilane (MPTMS)-coated glass slide attached to a motorized translation stage is immersed at a fixed rate into a 17 nM aqueous solution of 12-nm diameter colloidal Au, a gradient in particle coverage is generated in the direction of immersion. After sample rotation by 90°, fixed-rate immersion into a Ag⁺-containing solution designed to specifically deposit Ag on Au^{7b} leads to a gradient in particle size over the new immersion direction. The resulting surface exhibits a continuous variation in nanometer scale morphology—as defined by particle coverage and particle size—that results from known, repeatable immersion conditions.¹⁰ In our apparatus, a stepper motor with a 2° step yields a 3 μm translation. Over a 3 cm × 3 cm region, it is therefore possible to generate 10⁸ different, 9-μm² nanostructures. Macroscopic regions with uniform morphology can be prepared by very rapid successive steps followed by a long delay; these stepwise gradients are especially useful to probe bulk changes in physical properties. For example, optical changes linked to growth of the characteristic Ag plasmon band at 400 nm with increasing Ag coverage,⁷ evident to some degree in continuous gradient samples, are clearly visible as square regions with uniform color (supporting information).

The SERS signal for adsorbed *p*-nitrosodimethylaniline (*p*-NDMA) was measured over a 2 cm × 2 cm sample exhibiting continuous gradients in Au coverage and Ag cladding thickness. The immersion times for sample preparation (0–6 h for the Au gradient, 8–22 min for the Ag gradient) were established by determination of the most enhancing region from an initial, large gradient SERS screen on a 2 cm × 2 cm sample (0–12 h for Au, 0–30 min for Ag). Figure 1 shows a spatial map of the background-corrected SERS intensity¹¹ for the phenyl-nitroso stretch at 1168 cm⁻¹.¹² Intensity trends from 15 initial

* Author to whom all correspondence should be addressed: natan@chem.psu.edu.

[†] The Pennsylvania State University.

[‡] University of Pittsburgh.

(1) (a) Martin, E. J.; Blaney, J. M.; Siani, M. A.; Spellmeyer, D. C.; Wong, A. K.; Moss, W. H. *J. Med. Chem.* **1995**, *38*, 1431–1436. (b) Rohr, J. *Angew. Chem., Int. Ed. Engl.* **1995**, *34*, 881–885.

(2) Xiang, X.-D.; Sun, X.; Briceño, G.; Lou, Y.; Wang, K.-A.; Chang, H.; Wallace-Freedman, W. G.; Chen, S.-W.; Schultz, P. G. *Science* **1995**, *268*, 1738–1740.

(3) Briceño, G.; Chang, H.; Sun, X.; Schultz, P. G.; Xiang, X.-D. *Science* **1995**, *270*, 273–275.

(4) (a) Lee, A. F.; Baddeley, C. J.; Hardacre, C.; Ormerod, R. M.; Lambert, R. M. *J. Phys. Chem.* **1995**, *99*, 6096–6102. (b) Harada, M.; Asakura, K.; Toshima, N. *J. Phys. Chem.* **1993**, *97*, 5103–5114. (c) Szanyi, J.; Goodman, D. W. *J. Catal.* **1994**, *145*, 508–515.

(5) (a) Grabar, K. C.; Freeman, R. G.; Hommer, M. B.; Natan, M. J. *J. Anal. Chem.* **1995**, *67*, 735–743. (b) Grabar, K. C.; Allison, K. A.; Baker, B. E.; Bright, R. M.; Brown, K. R.; Dolan, C. M.; Freeman, R. G.; Fox, A. P.; Musick, M. D.; Natan, M. J. *Langmuir* **1996**, *12*, 2353–2361.

(6) See also: (a) Chumanov, G.; Sokolov, K.; Gregory, B. W.; Cotton, T. M. *J. Phys. Chem.* **1995**, *99*, 9466–9471. (b) Doron, A.; Katz, E.; Willner, I. *Langmuir* **1995**, *11*, 1313–1317.

(7) (a) Freeman, R. G.; Hommer, M. B.; Natan, M. J. *J. Phys. Chem.* **1996**, *100*, 718–724. (b) Bright, R. M.; Walter, D. G.; Musick, M. D.; Jackson, M. A.; Allison, K. J.; Natan, M. J. *Langmuir* **1996**, *12*, 810–817.

(8) (a) Brandt, E. S.; Cotton, T. M. In *Investigations of Surfaces and Interfaces-Part B*; 2nd ed.; Rossiter, B. W., Baetzold, R. C., Eds.; John Wiley & Sons: New York, 1993; Vol. IXB, Chapter 8, pp 633–718. (b) Birke, R. L.; Lu, T.; Lombardi, J. R. In *Techniques for Characterization of Electrodes and Electrochemical Processes*; Varma, R., Selman, J. R., Eds.; John Wiley & Sons: New York, 1991; Chapter 5, pp 211–277. (c) Moskovits, M. *Rev. Modern Phys.* **1985**, *57*, 783–826.

(9) Grabar, K. C.; Smith, P. C.; Musick, M. D.; Davis, J. A.; Walter, D. G.; Jackson, M. A.; Guthrie, A. P.; Natan, M. J. *J. Am. Chem. Soc.* **1996**, *118*, 1148–1153.

(10) The thickness of the Ag cladding is governed by the immersion time in the Ag⁺ solution, but it should be noted that the finite shelf life of commercial Ag plating formulations can lead to inconsistent deposition rates.

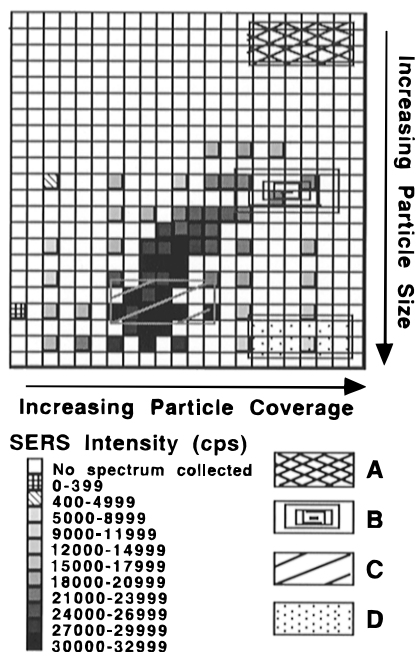


Figure 1. Background subtracted SERS intensity in counts per second (cps) for the 1168 cm^{-1} phenyl–nitroso stretch of p-NDMA as a function of sample position. Each shaded box represents one SERS spectrum collected in a $0.1\text{ cm} \times 0.1\text{ cm}$ area. Regions A–D correspond to AFM images in Figure 2. Experimental conditions: [p-NDMA] = 2.5 mM ; 30 mW of 647.1 nm photons focused to a $\approx 2\text{ mm}$ diameter spot at the sample; 1 cm^{-1} step, 1 s integration, 5 cm^{-1} band pass.

spots at 0.4-cm intervals were used to locate the most SERS-active area on the sample. Further interrogation at smaller intervals revealed a region that was greater than 10^2 -fold more enhancing than the least SERS-active domains of this substrate (and over 10^3 -fold more enhancing than the least active sites on the initial screen).

AFM was used to determine the nanometer-scale morphology at positions of interest (Figure 2).¹³ The image labels A–D correspond to representative morphologies at locations marked by shaded squares in Figure 1. Sampling positions were chosen to highlight variation in Ag cladding thickness (i.e. to span the vertical gradient) as opposed to variation in number density of particles. Accordingly, differences in particle coverage in images A, B, and D are not significant, and represent positional uncertainty in the horizontal (coverage) gradient. Immersion time in Ag^+ increases in the order $A < B < C < D$ ($A = 0\text{ min Ag}$), but SERS intensity follows the pattern $C > B > D > A$. Section analyses reveal that mean particle size increases from A to C as expected, but decreases in D.¹⁴ Two related effects contribute to this result: formation of small Ag particles between Ag-clad Au colloids, and loss of monolayer structure (i.e. formation of multilayers) upon extended Ag^+ exposure. This decrease in particle size can explain the diminished SERS signal from domain D relative to C, since smaller particles are less enhancing than larger ones.¹⁵ Alternatively, particle interconnection in D may be responsible for the decrease: there appears to be an optimum interparticle spacing defined by a narrow diagonal band of moderate Au particle coverage and Ag coating (Figure 1). A subtle interplay between particle size, shape, and spacing in SERS enhancements has previously been noted.⁸

Improvements in solution-based combinatorial assembly of metal surfaces will likely proceed along two lines. (i) Recently developed Raman imaging methods are intrinsically more

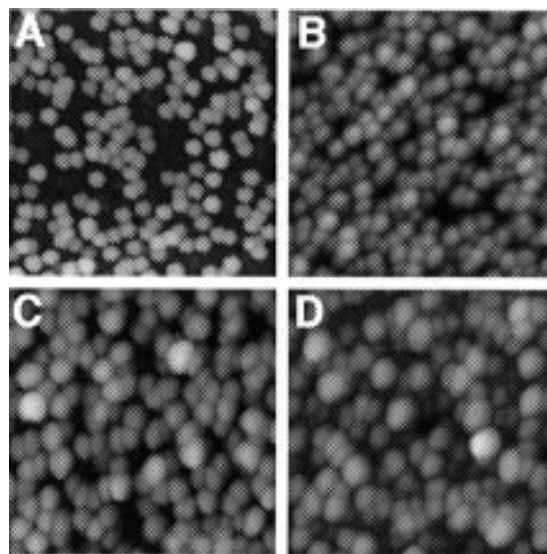


Figure 2. AFM images ($500\text{ nm} \times 500\text{ nm}$) of MPTMS-derivatized glass slides with varying coverages of 12-nm diameter colloidal Au and varying quantities of deposited Ag. Images A–D correspond to regions delineated in Figure 1. Z-axis (vertical) gray scale: black = 0 nm , white = 35 nm .

efficient than the laborious point-by-point mapping method described herein. With tunable filter imaging spectrometers¹⁶ and charge-coupled device detectors,¹⁷ it should be possible to probe up to 10^6 sample structures simultaneously. (ii) The ready availability of dispersible metal-containing nanoparticles¹⁸ and the numerous routes to metal deposition from complexed metal cations¹⁹ should allow extension of this method to a variety of other metals. These hypotheses are currently being tested.

Acknowledgment. Financial support from NSF (CHE 92–56692) and from the Beckman Foundation, a loan of equipment from Digital Instruments, and programming assistance from M. D. Musick are gratefully acknowledged.

Supporting Information Available: Three figures showing SERS spectra, a SERS intensity map of p-NDMA, and UV–vis spectra for different Au/Ag coatings (3 pages). See any current masthead page for ordering information and Internet access instructions.

JA961327W

(11) Samples for SERS were attached to an X–Y–Z micrometer mount for manual spatial manipulation. Spectra were acquired using a Spex 1404 scanning double monochromator fitted with a photomultiplier tube detector. Average background, taken from 1230 to 1240 cm^{-1} , was subtracted from the average peak intensity at 1168 – 1170 cm^{-1} for each spectrum. The spectral background ranged from 1000 to 5000 cps .

(12) Brazdil, J. F.; Yeager, E. B. *J. Phys. Chem.* **1981**, *85*, 995–1004.

(13) Data were acquired using a Digital Instruments Nanoscope III operated in tapping mode.

(14) (a) While sample-tip convolution leads to artificially large particle widths, height is an accurate measure of particle diameter.^{5b} (b) $A = 13\text{ nm}$; $B = 16\text{ nm}$; $C = 18\text{ nm}$; $D = 5$ – 18 nm .

(15) The effects of particle size-dependent changes in dielectric constants on SERS activity are described in: Zeman, E. J.; Schatz, G. C. *J. Phys. Chem.* **1987**, *91*, 634–643.

(16) (a) Schaeberle, M. D.; Karakarsanis, C. G.; Lau, C. J.; Treado, P. *J. Anal. Chem.* **1995**, *67*, 4316–4321. (b) Morris, H. R.; Hoyt, C. C.; Miller, P.; Treado, P. *J. Appl. Spectrosc.* **1996**, *50*, 805–811.

(17) Sweedler, J. V.; Ratzlaff, K. L.; Denton, M. B. *Charge-Transfer Devices in Spectroscopy*; VCH Publishers Inc.: New York, 1994.

(18) Examples: (a) Bradley, J. S. In *Clusters and Colloids, from Theory to Applications*; Schmid, G., Ed.; VCH: New York, 1994; pp 458–544. (b) Henglein, A. *Chem. Rev.* **1989**, *89*, 1861–1873.

(19) Examples: (a) Glavee, G. N.; Klabunde, K. J.; Sorensen, C. M.; Hadjipanayis, G. C. *Langmuir* **1994**, *10*, 4726–4730. (b) Reetz, M. T.; Helbig, W.; Quaiser, S. A. *Chem. Mater.* **1995**, *7*, 2227–2228.